Osman, A. S. *et al.* (2007). *Géotechnique* **57**, No. 9, 729–737 [**doi:** 10.1680/geot.2007.57.9.729]

Simple prediction of the undrained displacement of a circular surface foundation on non-linear soil

A. S. OSMAN*, D. J. WHITE†, A. M. BRITTO‡ and M. D. BOLTON†

Textbooks and university courses teach elasticity and plasticity as separate methods for analysing the stiffness and strength of a shallow foundation. The behaviour of real soil is neither linear elastic nor perfectly plastic. In this paper, two simple techniques for incorporating non-linearity in routine design have been validated using finite element (FE) analysis. These two techniques—Atkinson's method and the mobilisable strength design (MSD) approach—assume that the responses of an individual soil element and the boundary value problem being considered are self-similar. Using this assumption, the soil element response can be scaled to predict the response of the boundary value problem. Atkinson's method is based on elasticity whereas MSD uses plasticity. Non-linearity has been captured in the FE analysis using a power law soil model. This approach uses minimal parameters, but is shown to capture accurately the undrained stress–strain response of typical clays under monotonic loading. Comparison with elastic and plastic solutions showed that the FE analysis was accurate to within < 5% at the elastic and plastic extremes of the loading range. The responses of the soil and the boundary value problem are shown to be sufficiently self-similar up to two-thirds of the failure load for the foundation response to be predicted simply by a linear scaling of the soil response. Previously reported scaling factors for vertical loading are confirmed, and new factors for horizontal and moment loading are derived. These results show that, for this particular boundary value problem, soil non-linearity can be captured with sufficient accuracy for routine design, without recourse to sophisticated numerical analysis. These self-similarity methods are simple enough to be taught to undergraduates, and could be incorporated in textbooks alongside the core sections on elasticity and plasticity, providing guidance on the application of these techniques to real non-linear soil.

KEYWORDS: clays; deformation; design; footings/foundations; soil/structure interaction

Dans les livres de texte et les cours universitaires, on enseigne l'élasticité et la plasticité comme des méthodes distinctes d'analyse de la rigidité et de la résistance de fondations superficielles. Le comportement des sols réels ne présente pas une élasticité linéaire et n'est pas parfaitement plastique. Dans la présente communication, on a validé deux techniques simples d'incorporation de la non-linéarité dans les études courantes en utilisant l'analyse aux éléments finis. Ces deux techniques – la méthode d'Atkinson et la méthode d'étude à résistance mobilisable (MSD) – partent du principe que les réponses d'un élément du sol et le problème de la valeur limite à l'étude présentent une similitude intrinsèque. En appliquant cette hypothèse, il est possible d'extrapoler la réponse de l'élément du sol afin de prédire la réponse au problème de la valeur limite. La méthode d'Atkinson est basée sur l'élasticité, tandis que la méthode MSD fait usage de la plasticité. On a incorporé la non-linéarité dans l'analyse aux éléments finis en utilisant un modèle exponentiel du sol. Cette méthode fait usage de paramètres minimaux, mais elle démontre qu'elle est en mesure de saisir de façon précise la réponse à contrainte déformation sans consolidation d'argiles typiques sous charge monotone. La comparaison avec des solutions élastiques et plastiques a démontré que l'analyse aux éléments finis est précise à moins de 5% aux extrêmes élastiques et plastiques de la plage de charges. Les réponses du sol et le problème de la valeur limite présentent une similitude intrinsèque suffisante jusqu'à deux tiers de la charge de rupture pour la réaction des fondations pour qu'il soit possible de les prédire rien qu'avec une extrapolation linéaire de la réponse du sol. Les facteurs d'extrapolation indiqués précédemment pour les charges verticales sont confirmés, et on dérive des facteurs nouveaux pour la charge horizontale et à moment. Les résultats montrent que, pour ce problème de valeur limite particulier, on est en mesure d'obtenir la non-linéarité du sol avec une précision suffisante pour des études de routine, sans devoir recourir à une analyse numérique sophistiquée. Ces méthodes à similitude intrinsèque sont suffisamment simples pour être enseignées à des étudiants universitaires, et pourraient être incorporées dans des livres de texte conjointement avec les sections principales sur l'élasticité et la plasticité, en fournissant des indications sur l'application de ces techniques sur des sols non-linéaires réels.

INTRODUCTION

The load–displacement behaviour of a surface foundation resting on uniform soil is the most fundamental geotechnical boundary value problem. In undrained conditions the soil is often characterised by an elastic stiffness and an undrained strength. Using these soil parameters, established analytical solutions are available to calculate the stiffness and capacity of a circular surface foundation, under vertical, horizontal or moment loading. Linear elasticity is used to calculate stiffness, and plasticity theory is used to calculate capacity.

These elastic and plastic solutions, following the early work of Boussinesq (1885), Prandtl (1921) and others, are reproduced in every soil mechanics textbook, and lie within the core syllabus of almost every course on foundation engineering. However, the stress–strain response of soil is not linear-elastic perfectly plastic, but is highly non-linear within

Manuscript received 5 July 2006; revised manuscript accepted 27 June 2007.

Discussion on this paper closes on 1 May 2008, for further details see p. ii.

* School of Engineering, Durham University, UK.

† Schofield Centre, Department of Engineering, University of Cambridge, UK.

‡ IT Services Division, Department of Engineering, University of Cambridge, UK.

the strain range mobilised under typical working conditions. Therefore, despite the appealing analytical rigour of elasticity and plasticity, these theories cannot be applied in practice without some qualification. Linear elasticity can be applied to the calculation of settlement if the chosen value of secant stiffness is qualified by an estimate of the mobilised strain. Plasticity can be used to estimate the capacity of the foundation, and this load can be qualified by a large safety factor, which is assumed to limit settlements sufficiently.

Neither of these approaches takes rigorous account of the actual form of the non-linear stress–strain response, and the varying strain level within the deforming soil. There are two methods of including the actual stress–strain response in the design analysis. The first method is to use sophisticated numerical analysis—such as the finite element (FE) method—to simulate the non-linear response of every element of soil within the boundary value problem, and recover the resulting foundation behaviour. Until recently this approach was primarily a research tool, but it is anticipated that it will become more widely used in practice as computing power, training, and parameter selection methods improve (Potts, 2003).

The second approach to the inclusion of non-linearity in a design calculation is to use a simplified calculation method drawing on the concepts of elasticity and plasticity, and assuming that the element and the boundary value responses are self-similar. This assumption is bold—but proven in this paper for certain problems—and yields a calculation method that is far quicker and simpler than numerical analysis. This self-similarity approach can be within the framework of elasticity (e.g. Atkinson, 2000) or plasticity (e.g. Bolton, 1993).

The purpose of this paper is to demonstrate—using non-linear FE analysis—that for the case of a circular surface foundation on clay under vertical, horizontal or moment loading, soil non-linearity can be adequately captured using these simple self-similarity calculation methods. Only uniaxial monotonic loading is considered. The nomenclature used throughout the paper for foundation loading and displacement is shown in Fig. 1.

ELASTIC SOLUTIONS

For a foundation on a linear elastic half-space, the relationship between the applied vertical (V), horizontal (H) and moment (M) loads and the resulting displacements can be expressed in normalised matrix form as

$$\begin{Bmatrix} \dfrac{V}{GD^2} \\ \dfrac{H}{GD^2} \\ \dfrac{M}{GD^3} \end{Bmatrix} = \begin{bmatrix} K_v & & \\ & K_h & K_{mh} \\ & K_{mh} & K_m \end{bmatrix} \begin{Bmatrix} \dfrac{w}{D} \\ \dfrac{u}{D} \\ \theta \end{Bmatrix} \tag{1}$$

where K_v, K_h, K_m and K_{mh} are dimensionless elastic stiffness coefficients, which are dependent only on Poisson's ratio ν, the embedment conditions, and the foundation geometry. K_v, K_h and K_m correspond to vertical, horizontal and moment degrees of freedom respectively, K_{mh} describes any cross-coupling between the horizontal and moment degrees of freedom, and G is the shear modulus of the soil. The stiffness coefficients K_v, K_h, K_m and K_{mh} are obtained either analytically from elasticity theory or numerically using the finite element method (e.g. Bell, 1991; Ngo-Tran, 1996), aided by the scaled boundary method in the cases of Doherty & Deeks (2003) and Doherty *et al.* (2005). The cross-coupling stiffness coefficient K_{mh} is zero for surface circular footings (Bell, 1991).

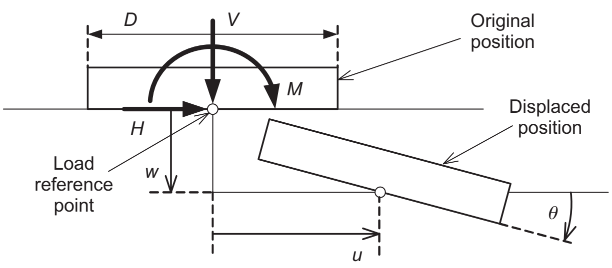

Fig. 1. Nomenclature for foundation loading and geometry

For a smooth rigid circular foundation on the surface of an elastic half-space, Poulos & Davis (1970) give closed-form solutions derived from elasticity theory for vertical and moment loading (assuming that tension can be sustained at the underside of the foundation). These solutions are exact for all values of Poisson's ratio. The stiffness coefficients K_v and K_m are

$$K_v = \frac{2}{1-\nu} \tag{2}$$

$$K_m = \frac{1}{3(1-\nu)} \tag{3}$$

For a rough rigid circular surface foundation, Spence (1968) gives an exact solution for vertical loading that can be written as

$$K_v = \frac{2\ln(3-4\nu)}{1-2\nu} \tag{4}$$

If the value of Poisson's ratio ν approaches 0·5, both equation (4) and equation (2) give a unique value of K_v, which is 4.0.

For horizontal loading there are two existing analytical solutions for the stiffness coefficient K_h, derived by Bycroft (1956)

$$K_h = \frac{16(1-\nu)}{7-8\nu} \tag{5}$$

and Gerrard & Harrison (1970)

$$K_h = \frac{4}{2-\nu} \tag{6}$$

Bell *et al.* (1991) demonstrate that both solutions are approximate, owing to additional assumed boundary conditions, except in the case of incompressible material (ν = 0·5), for which they are equal and exact. Bycroft's (1956) solution is based on the assumption that the foundation can only move in the horizontal direction. Gerrard & Harrison's (1970) solution does not satisfy the boundary conditions imposed by a rigid foundation, because it implies that the foundation is flexible in the vertical plane instead of rotating rigidly. No value of K_m for a rough foundation has been found in the literature, so the solution for a smooth foundation is used instead.

PLASTIC SOLUTIONS

The ultimate bearing capacity of a surface foundation is calculated using the Tresca failure criterion, in which the maximum shear stress is equal to the undrained strength, s_u. The limiting values of uniaxial load (i.e. applied in the absence of other loads) are denoted by bearing capacity factors as follows, where A is the surface area of the foundation, $\pi D^2/4$.

$$\frac{V}{As_u} = N_{cv} \tag{7}$$

$$\frac{H}{As_u} = N_{ch} \quad (8)$$

$$\frac{M}{ADs_u} = N_{cm} \quad (9)$$

Equal upper- and lower-bound plasticity solutions (Calladine, 1985) for the bearing capacity factor of a strip foundation under vertical load can be found analytically, giving $N_{cv} = (2 + \pi)$ (Prandtl, 1921). For circular geometry, a numerical solution scheme is required. Cox *et al.* (1961) present equal upper and lower bounds for a rough circular foundation, found using the method of characteristics, giving an exact solution of $N_{cv} = 6{\cdot}05$.

For uniaxial horizontal loading, ultimate failure is by sliding at the foundation/soil interface, so the horizontal bearing capacity factor is $N_{ch} = 1{\cdot}0$. Under pure moment loading, an upper-bound solution based on a spherical sliding surface beneath the foundation is presented by Murff & Hamilton (1993), giving a value of $N_{cm} = 0{\cdot}67$. No equivalent lower-bound solution is available, but this value is in good agreement with previous FE analyses (Gourvenec & Randolph, 2003), and so is likely to be close to the exact solution.

SOIL NON-LINEARITY

If soil exhibited linear elastic perfectly plastic behaviour, the elastic and plastic solutions presented above would be sufficient to (a) check the stability of a foundation, and (b) predict the settlement up to the load at which local plastic yielding occurs at the foundation edge, which for a strip foundation is $V/As_u = \pi$ (Bolton, 1979).

However, the stress–strain behaviour of soil is non-linear from very small strains (Jardine *et al.*, 1984; Burland, 1989; Houlsby & Wroth, 1991). The experimental work of Jardine *et al.* (1984) on low-plasticity clays shows that the region of purely elastic response rarely extends beyond 0·01% shear strain. Fig. 2 shows the variation of normalised shear modulus with strain in three different types of clay: Gault clay, London clay and kaolin clay. Fig. 2(a) shows the conventional plot of tangent shear modulus G reducing as the logarithm of shear strain increases during a triaxial compression test (Dasari, 1996). All three samples were sheared at an effective mean pressure p' of about 100 kPa. The overconsolidation ratios (OCR) of the Gault clay and London clay were 35 and 20 respectively. The kaolin clay was normally consolidated. Fig. 2(b) re-plots the data on log–log axes and shows that the three soils all closely follow the simple relation

$$\frac{G}{G_0} = \left(\frac{\varepsilon_q}{\varepsilon_{q0}}\right)^b \quad (10)$$

where G_0 is the small-strain elastic shear modulus, ε_q is the deviatoric strain, and ε_{q0} is the maximum deviatoric strain of linear elastic behaviour, at $\sim 10^{-5}$. The exponent $b = -0{\cdot}5$ fits the data of the three clays shown here.

Equation (10) can be rearranged and integrated to give a simple undrained ($\nu = 0{\cdot}5$) stress–strain relation in the form of a power law curve (for the range $\varepsilon_q > \varepsilon_{q0}$) in terms of the deviatoric stress q:

$$q = \frac{3G_0\varepsilon_{q0}}{b+1}\left[b + \left(\frac{\varepsilon_q}{\varepsilon_{q0}}\right)^{b+1}\right] \quad (11)$$

Power law curves have often been used to describe the stress–strain behaviour of soil (e.g. Gunn, 1993; Bolton & Whittle, 1999).

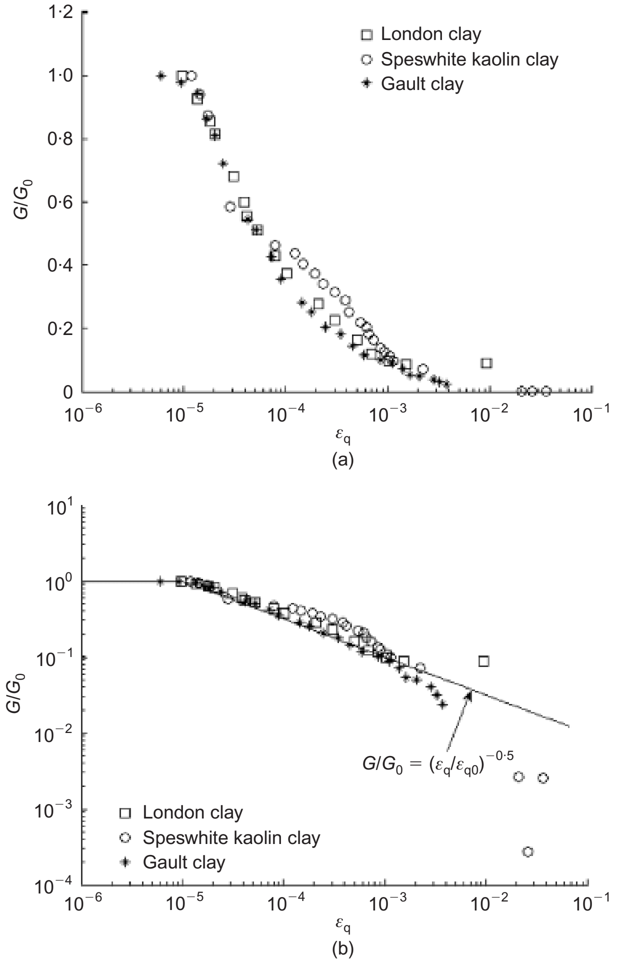

Fig. 2. Degradation of tangent stiffness with strain level for various clays (data adapted from Dasari, 1996): (a) normal scale; (b) logarithmic scale

ATKINSON'S METHOD

Atkinson (2000), in the 40th Rankine Lecture, described a calculation method that allows non-linearity to be considered in routine design, based on elasticity. He demonstrated this approach for the case of purely vertical loading on a circular foundation. Atkinson's method assumes that the decay in soil stiffness with strain level takes the same form as the decay in foundation stiffness with normalised settlement, w/D (Fig. 3). This form of self-similarity allows the strain axis of a plot of secant soil stiffness against strain to be linearly scaled to show

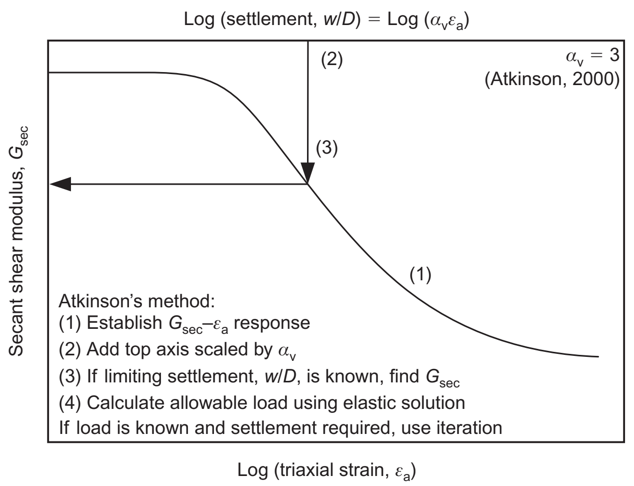

Fig. 3. Illustration of Atkinson's method

normalised settlement. The vertical axis remains unscaled, and shows the value of secant soil stiffness that should be used in a design calculation using the elastic solution (equations (2) and (4)). Based on comparison of model tests and triaxial compression tests, Atkinson (2000) suggests the apparent stiffness beneath a foundation at a settlement of w/D is equal to the secant stiffness in a triaxial test at a compressive strain of $\varepsilon_a = (w/D)/3$. In this paper, Atkinson's strain scaling factor for vertical displacement is denoted by $\alpha_v = (w/D)/\varepsilon_a = 3$. This value of α_v gave good agreement for centrifuge tests on stiff clay, in FE analysis for clay, and in calibration tests on sand (Atkinson, 2000). Application of Atkinson's method requires iteration if the load is known and the displacement is required. An initial equivalent linear stiffness is chosen (say $G_0/2$), leading to an elastic estimate of settlement under the design load $(w/D)_1$. This initial estimate of settlement allows a value of operative strain, $\varepsilon_{a,1} = (w/D)_1/3$, to be chosen, leading to a revised value of stiffness from the soil stiffness–strain relation. A second estimate of settlement can then be made, and the process is repeated until the required tolerance is reached. If the maximum load that will not exceed a limiting settlement is required, Atkinson's method does not involve iteration (Fig. 3).

THE MOBILISABLE STRENGTH DESIGN (MSD) APPROACH

Bolton (1993) described a design approach that allows non-linearity to be considered in a routine calculation, based on plasticity. Osman & Bolton (2005) demonstrated this approach for the case of purely vertical loading on a circular foundation, and termed this method 'mobilisable strength design' (MSD). In common with Atkinson's method, MSD assumes that the responses of the soil and boundary value problem are self-similar. However, instead of using an elastic solution to link soil stiffness to the stiffness of the boundary problem, plasticity is used to scale the stress–strain axes into load–displacement, as shown in Fig. 4. The stress axis is converted to load by multiplying by the bearing capacity coefficient N_c. The strain axis is converted to displacement by dividing by a compatibility factor M_c. This factor gives the ratio between the average shear strain within the deforming soil and the normalised displacement of the foundation. Osman & Bolton (2005) analysed the case of vertical loading of a rigid circular foundation, and derived M_{cv} analytically using an upper-bound plasticity solution. The chosen solution is not exact—it gives a value of N_{cv} that lies 3% above the exact solution—but it includes only distributed shear (rather than slip planes), so the shear strain rate is finite throughout the deforming soil, allowing an average value to be calculated. Osman & Bolton's compatibility factor M_{cv} is equal to 1·35 in the case of a smooth circular footing.

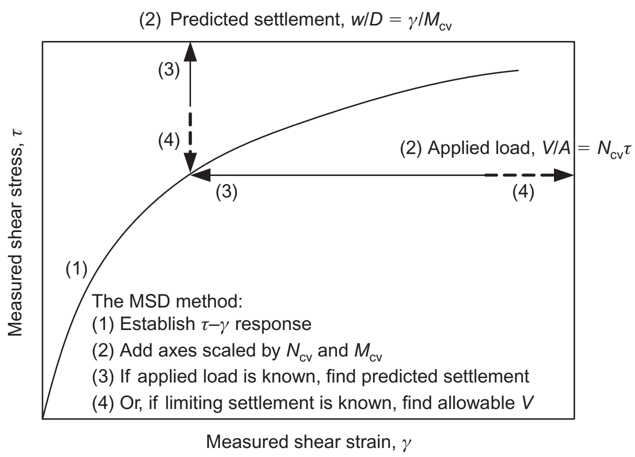

Fig. 4. Illustration of the MSD approach

In this paper Atkinson's method and MSD are compared for the case of a rough rigid circular foundation on non-linear soil representative of undrained clay, using FE analysis. The methods are extended to the cases of horizontal or moment loading, and additional strain scaling factors α_h and α_m and compatibility factors M_{ch} and M_{cm} are derived numerically.

FINITE ELEMENT MODEL

Constitutive model

Finite element analyses were carried out using ABAQUS/Standard version 6·5 software (HKS, 2003). A very simple approach has been used to represent the non-linearity of the stress–strain behaviour of soil. The undrained material response of the soil was represented with a non-linear perfectly plastic constitutive model, of the form described by Gunn (1993). This model uses a simple power law to represent the decay of soil stiffness with increasing strain. The non-linear undrained response of the soil is given by equation (11). At very small strain ($\varepsilon_q < 10^{-5}$) the soil stiffness is assumed to be constant and equal to the tangent stiffness given by the power law at $\varepsilon_q = 10^{-5}$.

The soil is assumed to yield according to the Tresca failure condition, with the maximum shear stress in any plane limited to the undrained shear strength s_u. In order to avoid problems in defining the relative plastic strain magnitudes at the vertices of the hexagonal Tresca failure criterion, the direction of plastic strain increments at the vertices is calculated using the Von Mises flow rule.

Finite element mesh

The purpose of the FE analyses reported in this paper is to calculate the load–displacement response of footings under each uniaxial loading condition—vertical, horizontal and moment—and assess whether Atkinson's method and MSD can capture this response. The validity of the FE results is assessed by (a) comparing the initial linear part of the load–displacement response with the elastic solutions given by equations (1)–(6), and (b) comparing the limit loads with the plastic solutions given by equations (7)–(9).

The elastic solutions apply to an unbounded half-space, and the region of significant load and deformation is a small part of the domain. This unbounded region can be approximated by extending the FE mesh to a great distance, so that the influence of the boundaries on the region of interest is minimal. This approach requires a large mesh. Bell (1991) studied the effect of mesh dimensions on FE results for a circular footing using two-dimensional axisymmetric meshes of six-noded triangular elements. The linear elastic FE analysis gave an error of 10·3% in the vertical stiffness coefficient K_v compared with the closed-form solution when using an FE mesh of dimensions $5D \times 5D$. This error reduced to 2·4% using a $25D \times 25D$ mesh and to 1·1% with a $100D \times 100D$ mesh. Bell (1991) also carried out three-dimensional FE analyses with 20-noded quadratic strain tetrahedron elements and a $100D \times 100D$ mesh and obtained errors that ranged from 2·5% to 3·9% for $\nu = 0$ to 0·49.

An alternative approach to the extension of the FE mesh to account for the boundary is to use 'infinite elements'. These elements are defined over semi-infinite domains with suitably chosen decay functions. The Abaqus software provides infinite elements for static response based on the formulations of Zienkiewicz *et al.* (1983).

The three-dimensional FE mesh used in the present analysis is shown in Fig. 5, and represents a semi-cylindrical

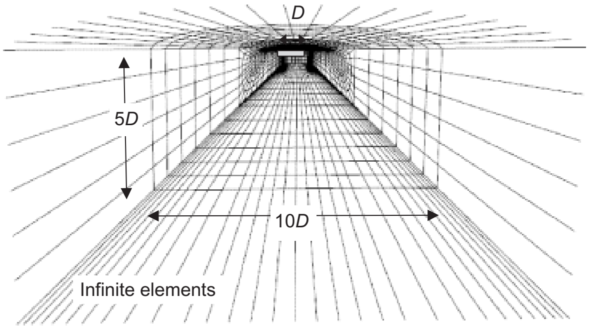

Fig. 5. Geometry of FE mesh

section through a diametrical plane of a circular footing of diameter *D*. The mesh comprises 20-noded reduced integration quadratic continuum elements forming a core of radius 5*D* and a depth of 5*D* surrounded by infinite elements modelling the far-field region. The Abaqus formulations require that these elements extend a distance equal to the extent of the region of continuum elements away from the centreline. Displacement boundary conditions prevent out-of-plane displacements along the plane of symmetry (i.e. the flat diametrical plane on the face of the mesh). The footing was modelled as a rigid body with full bonding at the soil/footing interface. The mesh comprises a total of 15 090 elements and 63 353 nodes, and was fine near the footing where the stress and the strain gradients are high. Intense discretisation of the mesh was provided near the interface with the footing edges, with rows of elements less than 0·01*D* in depth and columns of elements less than 0·025*D* in width. Gourvenec & Randolph (2003) show that this refinement provides appropriate kinematics for vertical, horizontal and moment loading.

Loading method and constitutive parameters

Only uniaxial loading is considered in this paper. Separate analyses applying load in the vertical, horizontal and moment direction were conducted. Increments of loading were applied at the load reference point (Fig. 1), corresponding to $< 1\%$ of the ultimate load in each case.

The exponent parameter *b* in equation (8) is taken to be $-0{\cdot}5$, which is consistent with the data shown in Fig. 2. The small-strain rigidity ratio G_0/s_u is taken to be 1054. The limit of linear elastic behaviour is a shear strain of $\varepsilon_{q0} = 10^{-5}$. This combination of parameters leads to mobilisation of the maximum undrained strength at a deviatoric strain of 1%, and gives a good fit to the data for various clays shown in Fig. 2. All the analyses were carried out with Poisson's ratio $\nu = 0{\cdot}49$, corresponding to nearly incompressible material. A value of $\nu = 0{\cdot}49$ is used instead of exactly 0·5, which avoids numerical difficulties, and introduces only small but acceptable errors into the solution (Potts & Zdravkovic, 1999).

A triaxial compression test on this model soil was simulated using a single eight-noded quadratic axisymmetric finite element, with horizontal freedom to simulate frictionless platens.

FINITE ELEMENT RESULTS

Results expressed as stress–strain and load–displacement

Figure 6 shows the results of FE calculations for a triaxial sample and for rough circular surface foundations under vertical load, horizontal load, and moment. The stress–strain curve for the triaxial sample is plotted on q/q_{ult}:ε_q axes and agrees with the defined constitutive relation given by equation (11). The behaviour of the foundations is also plotted as normalised load (V/V_{ult}, H/H_{ult} or M/M_{ult}) against displacement ratio (w/D, u/D, or θ). All three curves approach an ultimate load (or stress) at large strains or displacements.

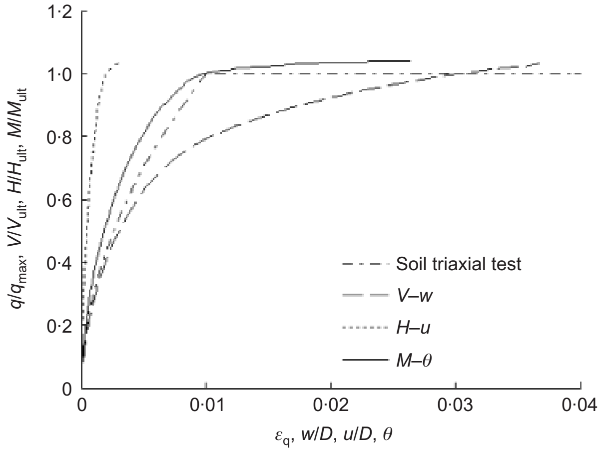

Fig. 6. Stress–strain curve and shallow foundation load–displacement response from FE analysis

Results expressed as stiffness–strain and stiffness–displacement

From the load–displacement curves in Fig. 6, the variation in secant stiffness is calculated from equation (1) using the appropriate stiffness coefficients. For the case of vertical load, the stiffness coefficient K_v is calculated from equation (4):

$$G = \frac{V}{D^2 K_v (w/D)} = \frac{V(1-2v)}{2Dw \ln(3-4v)} \tag{12}$$

The stiffness coefficient K_h is calculated from equation (5):

$$G = \frac{H}{D^2 K_h (u/D)} = \frac{H(7-8v)}{16Du(1-v)} \tag{13}$$

Since there is no analytical solution for rough footings subject to moments, the stiffness coefficient K_m derived for smooth footings is used:

$$G = \frac{M}{D^3 K_m \theta} = \frac{3M(1-v)}{D^3 \theta} \tag{14}$$

A Poisson's ratio of 0·49 is used in the back-calculation of the secant stiffness for consistency with the FE analyses.

Figure 7 shows the back-calculated secant stiffness from each mode of loading, normalised by the initial soil stiffness, plotted against the corresponding normalised displacements (w/D, u/D, θ). This figure also shows the soil secant stiffness plotted against deviatoric strain, which agrees with the specified constitutive relation given by the elastic region followed by the non-linear response of equation (10).

In the very small strain range ($\varepsilon_q < 10^{-5}$), the soil responds linearly and all modes of loading show a back-calculated operative stiffness of G_0. In the range of non-linear behaviour ($\varepsilon_q > 10^{-5}$), each mode of loading shows a different rate of stiffness degradation with strain, in the same way that each mode of loading showed a different shape of load–displacement response in Fig. 6.

Comparison with elastic and plastic solutions

The initial operative soil stiffness back-calculated according to equations (12)–(14) can be compared with the

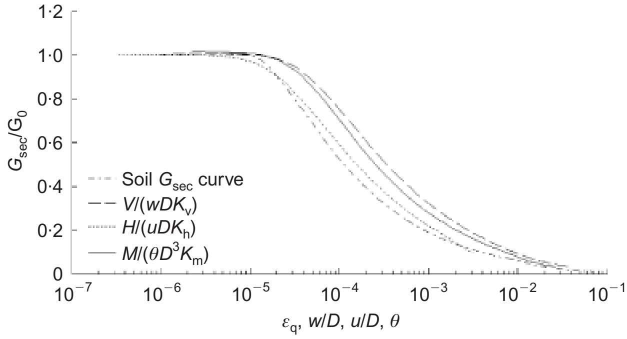

Fig. 7. Secant stiffness degradation for soil element and shallow foundation from FE analysis

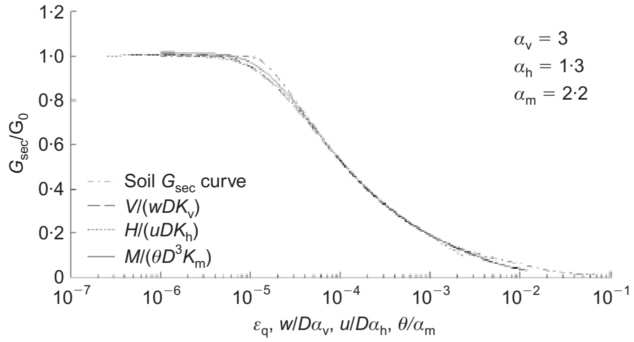

Fig. 8. Comparison of soil element and foundation response using Atkinson's method

specified value of G_0 to assess the accuracy of the early part of the FE load–displacement response. The bearing capacity factor mobilised in the final load step that could achieve equilibrium can be compared with the theoretical bearing capacity factors to assess the accuracy of the final part of the load–displacement response. Table 1 shows that, within the elastic range, the FE results lie within 1·38% of the theoretical solutions. In the final load steps, the theoretical bearing capacity factors are exceeded by 3·3–4·5%, which is slightly higher than found by Gourvenec & Randolph (2003) using a similar mesh (but under displacement rather than load control), but still acceptably small.

The small errors in the predicted bearing capacity factors can be attributed partly to mesh distortion, which will not influence the earlier part of the response under low mobilised load. For this reason, the theoretical values of ultimate uniaxial load have been used to calculate normalised values of load (V/V_{ult}, H/H_{ult} and M/M_{ult}), rather than the measured ultimate values.

DISCUSSION

Interpretation following Atkinson's method

The horizontally scattered curves in Fig. 7 can be brought together by scaling the displacement data in the manner used by Atkinson's method. In Fig. 8, the normalised vertical displacement has been adjusted according to Atkinson's strain scaling factor $\alpha_v = 3$. The vertical response now overlies the soil response. After scaling in this fashion, the soil response represents a prediction of the vertical response found by Atkinson's method (but scaled by $1/\alpha_v$), while the vertical response represents the actual behaviour, according to the FE analysis (also scaled by $1/\alpha_v$). The close agreement of these two curves is consistent with Atkinson's (2000) observations from centrifuge test results and finite element analyses that led to the proposal of $\alpha_v = 3$.

To extend Atkinson's method to horizontal and moment loading, strain scaling factors of $\alpha_h = 1{\cdot}3$ and $\alpha_m = 2{\cdot}2$ have been used to unite the corresponding foundation responses with the soil element response; these curves are also shown in Fig. 8. The good agreement between the four curves in Fig. 8 implies that the foundation responses in the different modes of loading are similar in shape to the soil stiffness, and can be derived according to Atkinson's method.

α_h is significantly lower than both α_m and α_v, implying that the development of local plastic yielding—leading to a degradation in back-calculated stiffness—occurs at a lower normalised displacement under horizontal loading, compared with moment or vertical loading.

Interpretation following the MSD approach

Figure 9 shows the mobilised soil strength and the normalised loads plotted against strain and normalised displacements scaled using compatibility factors to fit the engineering shear strain γ to the displacements consistent with the style of the MSD method (note that $\gamma = 1{\cdot}5\varepsilon_q$). After scaling in this fashion, the soil response represents an MSD prediction of the foundation response, on whichever axes are chosen (V–w, H–u or M–θ), while the FE results show the actual response. The M_{cv} factor of 1·35 derived analytically for smooth footing by Osman & Bolton (2005) united the vertical response of a smooth foundation with the soil response. This agreement confirmed that the upper-bound plasticity solution used to derive this compatibility

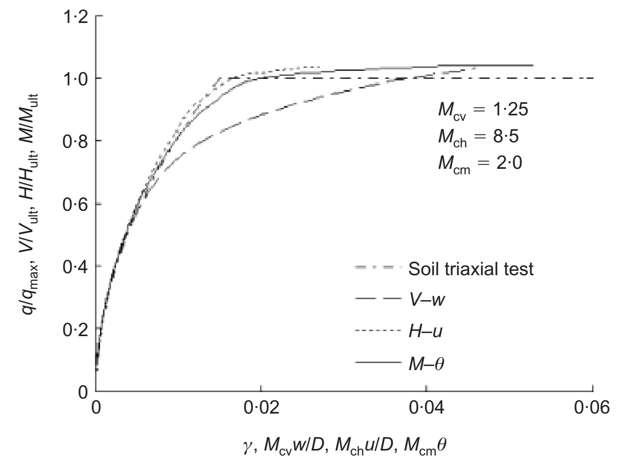

Fig. 9. Comparison of soil element and foundation response using the MSD approach

Table 1. Comparison of the elastic and plastic solutions and the FE results

Loading direction	Vertical	Horizontal	Moment
Error in back-calculated G_0: %	0·65	0·42	1·38
Calculated bearing capacity factor	$N_{cv} = 6{\cdot}25$	$N_{ch} = 1{\cdot}04$	$N_{cm} = 0{\cdot}70$
Theoretical bearing capacity factor	$N_{cv} = 6{\cdot}05$	$N_{ch} = 1{\cdot}00$	$N_{cm} = 0{\cdot}67$
Error in bearing capacity factor: %	3·3	3·8	4·5

factor, although not the strictly exact solution (instead giving a value of N_{cv} that is 3% above the true solution), provided an appropriate compatibility factor for use in the MSD approach. However, a compatibility factor M_{cv} of 1·25 is preferred in the current analysis of a rough foundation, mainly because this value will be shown to give a slightly conservative prediction in the range of practical interest.

To unite the foundation response under horizontal and moment loading with the soil element response, compatibility factors of $M_{ch} = 8{\cdot}5$ and $M_{cm} = 2{\cdot}0$ are used. The M_{ch} value is considerably higher than M_{cv}, since the zone of influence of the displacements is much smaller in the case of horizontal loading than in the case of vertical loading. Excellent agreement is shown between the scaled MSD curves and the soil response up to a load factor—defined as the applied load divided by the ultimate capacity—of 0·67. Higher load factors are rare in practice, so the agreement spans the entire range of relevant behaviour. The successful MSD normalisation shown in Fig. 9 echoes the conclusion from Fig. 8. The responses of the soil and of the foundation are self-similar, so useful predictions of the foundation displacement can be made by directly scaling the soil response.

Comparison of Atkinson's method and MSD

The results shown in Figs 8 and 9 can be re-plotted as the ratio of the numerical FE result and the prediction based on the two simple methods, as a function of load factor. In Fig. 10(a), the ratio of the secant stiffness from Atkinson's method to the FE result is shown for each mode of loading. In Fig. 10(b), the ratio of the displacement in the FE analysis to the MSD prediction is shown. These two ratios are directly comparable, because the displacement predicted in Atkinson's elastic method is inversely proportional to the secant stiffness. For both ratios, a value greater than unity indicates that the simple design method underpredicts the displacement, which is usually unconservative. Fig. 11 repeats Fig. 10 using normalised displacements as the horizontal axis.

Both Atkinson's method and the MSD approach provide displacement predictions that are accurate to within 20% for load factors in the range 0·2–0·67 (corresponding to a 'factor of safety' in the range 1·5–5). This accuracy is sufficient for routine foundation design. It is likely that there will be far greater uncertainty in the choice of design soil response. The discrepancy following the MSD method is larger than with Atkinson's method. The underprediction of displacement below a load factor of 0·2, where the relative displacement is of the order of 1/5000, is not of much practical significance. The underprediction of displacement above a load factor of 0·67 is also relatively unimportant, because this carries the foundation beyond acceptable working loads.

MSD would be expected to depend for its accuracy on the self-similarity of the stress–strain curves at any stress level and therefore to be most reliable for pure power curves. In the current paper, the FE simulations were conducted on soil obeying a power curve in its middle range but with stiffness reduced at very small strain (the G_0 cut-off) and at large strain (the s_u cut-off). It is therefore understandable that MSD underpredicts foundation displacements where stress concentrations cause the boundary value problem to 'cut the corner' of these kinks in the stress–strain curve. Discontinuities in tangent stiffness provide the sternest test for predictions based on self-similarity, such as by using MSD.

This paper has extended and verified two simple methods for predicting the undrained displacement of a circular surface foundation. The two methods are based on the assumption of self-similarity—as outlined in Figs 3 and 4—and the required scaling factors are summarised in Table 2. It should be noted that the non-linear soil response means that superposition, for example of vertical load and moment loading, cannot be used. Fresh factors would have to be derived for Table 2 to cover cases of combined loading.

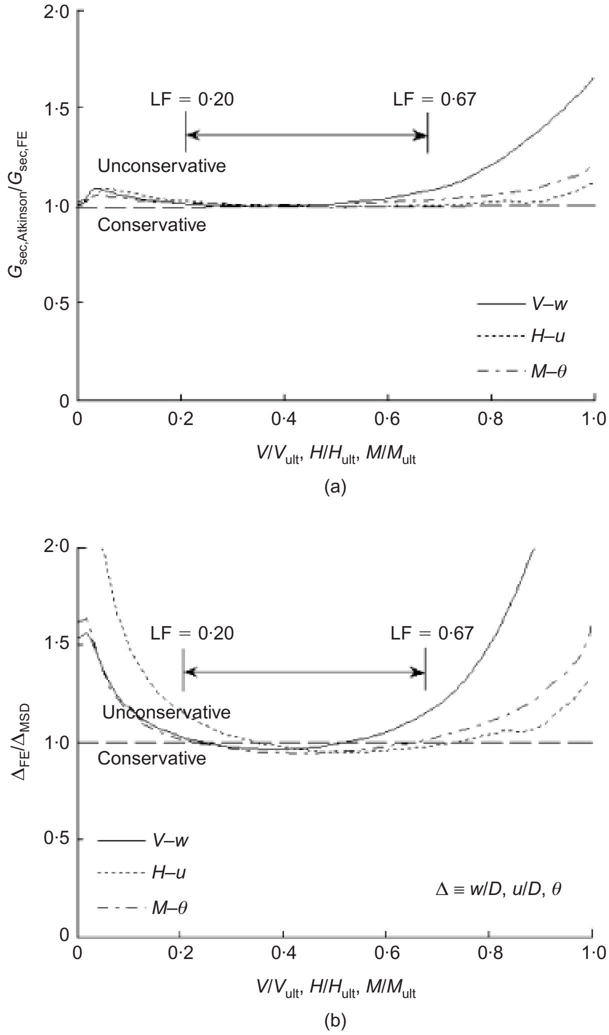

Fig. 10. Accuracy of Atkinson's method and the MSD approach expressed in terms of load factors (LF): (a) Atkinson's method; (b) MSD approach

CONCLUSIONS

Textbooks and university courses teach elasticity and plasticity as separate methods for analysing the response of a shallow foundation to applied load. Elasticity is for calculating settlement, and plasticity is for calculating ultimate capacity. However, the behaviour of real soil is neither linear-elastic nor perfectly plastic under typical working loads.

In this paper, the load–displacement behaviour of a surface foundation resting on soil with a non-linear stress–strain response has been investigated using FE analysis. The aim was to establish whether two simple methods, based on elasticity (Atkinson's method) and on plasticity (the MSD method), can be used to capture the full non-linear foundation response during uniaxial loading in different directions. These two methods assume that the responses of an individual soil element and the entire boundary value problem are self-similar. Using this assumption, the soil element response can be scaled to predict the response of the boundary value problem. Atkinson's method uses elastic solutions to link load

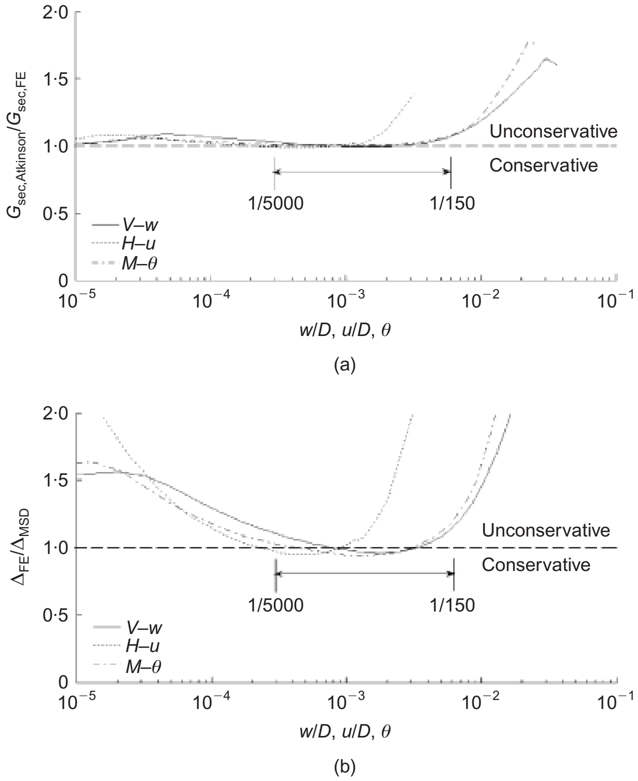

Fig. 11. Accuracy of Atkinson's method and the MSD approach expressed in terms of normalised displacements: (a) Atkinson's method; (b) MSD approach

and displacement via an appropriate secant stiffness. Linear scaling is used to link the soil strain and the normalised displacement, in order to identify the operative secant stiffness. The MSD method uses concepts of plasticity to scale directly from axes of stress and strain to load and displacement.

Non-linear FE analysis has been conducted using a truncated power law model to capture the non-linear undrained response of clay. This approach uses minimal parameters, but is shown to capture accurately the stress–strain response of typical clays. The very dense FE mesh used infinite elements to eliminate boundary effects, and was compared with elastic and plastic solutions to check accuracy. During initial loading, the maximum deviation from the elastic solution was found to be 1·38%, and at failure the applied load differed from the theoretical ultimate capacity by $<$ 5%.

Atkinson's approach relating the design stiffness, back-calculated from the settlement of the footing, to the soil stiffness degradation curve was validated by the FE results. This approach was extended to the cases of horizontal loading and moment loading by the derivation of new strain scaling factors. The MSD approach was also validated, by good agreement between the predicted and back-analysed results. New compatibility factors to scale the soil strain response into normalised horizontal and rotational movement were derived. These compatibility factors, together with previously published bearing capacity factors, allow the load–displacement behaviour to be predicted by scaling directly from a stress–strain curve.

Both Atkinson's method and the MSD approach provide predictions that are accurate to within 20% for typical working loads. These results show that good predictions of non-linear foundation behaviour can be made directly from the soil element response, using two simple methods, based on elasticity and plasticity. These methods rely on the assumption that the responses of the soil and the boundary value problem are self-similar, which has been confirmed by numerical analysis for the case of a surface foundation.

The consideration of soil non-linearity in routine design is therefore possible for this particular boundary value problem, without recourse to sophisticated numerical analysis. These self-similarity methods are sufficiently simple to be taught at undergraduate level, and could be incorporated in textbooks alongside the core sections on elasticity and plasticity, providing an explanation as to how these solutions can be applied to real non-linear soil.

ACKNOWLEDGEMENTS

The authors acknowledge the support of the Engineering and Physical Sciences Research Council (EPSRC): Platform Grant GR/T 18660/01 and the Royal Society (Research Grant: 2006/R2).

NOTATION

A foundation area, $\pi D^2/4$
b parameter describing power law decay of shear stiffness
D foundation diameter
G elastic shear modulus
G_0 small-strain elastic shear modulus
H horizontal load
K dimensionless stiffness coefficient
M moment load
M_c compatibility factor
N_c bearing capacity factor
q deviatoric stress ($q = \sqrt{\frac{3}{2} s_{ij} s_{ij}}$, $s_{ij} = \sigma_{ij} - \sigma_{kk}\delta_{ij}/3$)
s_u undrained soil strength
u horizontal foundation displacement
V vertical load
w vertical foundation displacement
α strain scaling factor in Atkinson's method
γ engineering shear strain
ε_a triaxial compression strain
ε_q deviatoric strain ($\varepsilon_q = \sqrt{\frac{2}{3}\varepsilon_{ij}\varepsilon_{ij}}$, i, j principal directions)
ε_{q0} deviatoric strain at limit of elastic behaviour
θ foundation rotation

Table 2. Derived scaling factors for the response of a rough circular surface foundation

Axis	Atkinson's method	Mobilisable strength design (MSD)
Load	–	Vertical: $N_{cv} = 6{\cdot}05$ Horizontal: $N_{ch} = 1{\cdot}0$ Moment: $N_{cm} = 0{\cdot}67$
Stiffness	Equations (2)–(6)	–
Displacement	Vertical: $\alpha_v = 3$ Horizontal: $\alpha_h = 1{\cdot}3$ Moment: $\alpha_m = 2{\cdot}2$	Vertical: $M_{cv} = 1{\cdot}25$ Horizontal: $M_{ch} = 8{\cdot}5$ Moment: $M_{cm} = 2{\cdot}0$

Subscripts

h horizontal
m moment (rotational)
v vertical
ult ultimate

REFERENCES

Atkinson, J. H. (2000). Non-linear soil stiffness in routine design. *Géotechnique* **50**, No. 5, 487–508.

Bell, R. W. (1991). *The analysis of offshore foundations subjected to combined loading*. MSc dissertation, Oxford University.

Bell, R. W., Houlsby, G. T. & Burd, H. J (1991). Finite element analysis of axisymmetric footings subjected to combined loads. *Proceedings of the international conference on computer methods and advances in geomechanics*, Cairns, Australia, Vol. 3, pp. 1765–1770.

Bolton, M. D. (1979). *A guide to soil mechanics*. London: Macmillan.

Bolton, M. D. (1993). Design methods. In *Predictive soil mechanics, Proceedings of Wroth Memorial Symposium*, pp. 50–72. London: Thomas Telford.

Bolton, M. D. & Whittle, R. W. (1999). A non-linear elastic/perfectly plastic analysis for plane strain undrained expansion. *Géotechnique* **49**, No. 1, 133–141.

Boussinesq, J. (1885). *Applications des potentials à l'étude d'équilibre et du movement des solides élastiques*. Paris : Gauthier Villars.

Burland, J. B. (1989). Small is beautiful: the stiffness of soils at small strains: Ninth Laurits Bjerrum Memorial Lecture. *Can. Geotech. J.* **26**, No. 4, 138–143.

Bycroft, R. N. (1956). Forced vibrations of a rigid circular plate on a semi-infinite elastic space and on elastic stratum. *Phil. Trans. R. Soc. London A* **248**, 327–368.

Calladine, C. R. (1985). *Plasticity for engineers*, 1st edn. Chichester: Ellis Horwood.

Cox, A. D., Eason, G. & Hopkins, H. G. (1961) Axially symmetric plastic deformation of soils. *Proc. R. Soc. London A* **254**, 1–45.

Dasari, G. R. (1996). *Modelling the variation of soil stiffness during sequential construction*. PhD dissertation, University of Cambridge.

Doherty, J. P. & Deeks, A. J. (2003). Elastic response of circular footings embedded in a non-homogeneous half-space. *Géotechnique* **53**, No. 8, 703–714.

Doherty, J. P., Houlsby, G. T. & Deeks, A. J. (2005). Stiffness of flexible caisson foundations embedded in nonhomogeneous elastic soil. *ASCE J. Geotech. Geoenviron. Engng* **131**, No. 12, 1498–1508.

Gerrard, C. M. & Harrison, W. J. (1970). *Circular loads applied to a cross-anisotropic half space*, Technical paper No. 8. CSIRO Division of Applied Geomechanics.

Gourvenec, S. & Randolph, M. (2003). Effect of strength non-homogeneity on the shape of failure envelopes for combined loading of strip and circular foundations on clay. *Géotechnique* **53**, No. 6, 575–586.

Gunn, M. J. (1993). The prediction of surface settlement profiles due to tunneling. In *Predictive soil mechanics, Proceedings of Wroth Memorial Symposium*, pp. 304–314. London: Thomas Telford.

HKS (2003). *ABAQUS/Standard user's manual, version 6·5*. Pawtucket, RI: Hibbit, Karlsson & Sorensen Inc.

Houlsby, G. T. & Wroth, C. P. (1991). Variation of shear modulus of a clay with pressure and overconsolidation ratio. *Soils Found.* **31**, No. 3, 138–143.

Jardine, R. J., Symes, M. J. & Burland, J. (1984). The measurement of soil stiffness in the triaxial apparatus. *Géotechnique* **34**, No. 3, 323–340.

Murff, J. D. & Hamilton, J. M. (1993) P-ultimate for undrained analysis of laterally loaded piles. *ASCE J. Geotech. Engng Div.* **119**, No. 1, 91–107.

Ngo-Tran, C. L. (1996). *The analysis of offshore foundations subjected to combined loading*. DPhil dissertation, Oxford University.

Osman, A. S. & Bolton, M. D. (2005). Plasticity based method for predicting undrained settlement of shallow foundations on clay. *Géotechnique* **55**, No. 6, 435–447.

Potts, D. M. (2003). Numerical analysis: a virtual dream or practical reality? *Géotechnique* **53**, No. 6, 535–573.

Potts, D. M. & Zdravković, L. (1999). *Finite element analysis in geotechnical engineering: Theory*, 1st edn. London: Thomas Telford.

Poulos, H. G. & Davis, E. H. (1970). *Elastic solutions for soil and rock mechanics*. New York: John Wiley & Sons.

Prandtl, L. (1921). Eindringungsfestigkeit und festigkeit von schneiden. *Angew. Math. U. Mech.* **1**, 15–20.

Spence, D. A. (1968). Self similar solutions to adhesive contact problems with incremental loading. *Proc. R. Soc. London A* **305**, 55–80.

Zienkiewicz, O. C., Emson, C. & Bettess, P. (1983). A novel boundary infinite element. *Int. J. Numer. Methods Engng* **19**, No. 2, 393–404.